AAE 462

Mission B: Lunar Payload Delivery

Preliminary Design Report

Cahleal Walker, Oliver Braitsch, Alejadro Esteva, Clay Mcleod

March 19, 2026

Executive Summary

The mission B option is interpreted, designed, and planned out in this document. The goal of this mission is to transport a 50-kilogram science instrument from a 400 km Low Earth Orbit to 100 km circular low lunar Orbit, using a vehicle with a restartable upper stage.

This mission consists of two different phases, including a Trans-Lunar Injection (TLI), a coast phase with trajectory corrections, and a Lunar Orbit Insertion (LOI). The total mission ΔV requirement is 4.076 km/s, including 3.107 km/s for TLI, 0.819 km/s for LOI, and 0.150 km/s of margin. A two-stage configuration was selected because a staging trade study showed that the two-stage configuration reduced the initial mass by 25.15% compared to a single-stage design.

The final vehicle uses a LOX/RP-1 pump-fed first stage for TLI and a pressure-fed, restartable NTO/MMH upper stage for LOI and maneuvering. The ΔV is allocated as 3.107 km/s for Stage 1 and 0.969 km/s for Stage 2. The total initial mass in LEO is 229.75 kg, including 161.55 kg propellant, 18.20 kg structure, and the 50 kg payload. Additionally, the propulsion systems for stages 1 and 2 produce a thrust of approximately 1620.20 N and 241.67 N, with specific impulses of 332 s and 304 s, respectively.

Ideal trajectory analysis shows that the spacecraft reaches the moon with an excess ΔV of approximately 0.278 km/s, which corresponds to approximately 63 seconds of burn time available for both trajectory corrections and mission operations.

At the system level, our design demonstrates strong consistency between mission analysis, propulsion performance, thermochemistry, and mass sizing. The LOX/RP-1 first stage enables an efficient high-energy transfer, while the hypergolic NTO/MMH upper stage ensures reliable restart capability after coast phases. Overall, the vehicle meets mission requirements with a mass-efficient and realistic design that is capable of delivering the 50 kg payload to lunar orbit with adequate margins.

1. Mission Analyst & Vehicle Architect (Role 1)

1.1 Mission Overview

The objective of this mission is to deliver a 50 kg payload from a 400 km circular Low Earth Orbit (LEO) to a 100 km circular lunar orbit that utilizes a restartable upper stage.

The mission trajectory consists of three primary components:

1. Trans-Lunar Injection (TLI)
2. Coast phase and midcourse corrections
3. Lunar Orbit Insertion (LOI)

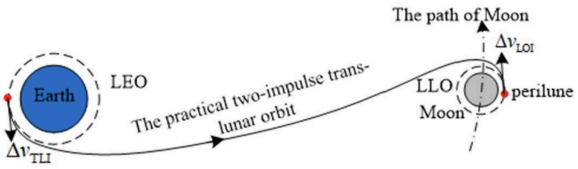

Figure 1. Translunar transfer from Low Earth Orbit to low lunar orbit. [1]

1.2 ΔV Budget Breakdown

A preliminary ΔV budget was constructed using values from NASA mission documentation. For the TLI and LOI burns, values from NASA's COMPASS Lunar Lander Study were used as representative estimates [2].

1. Trans-Lunar Injection: $\Delta V_{TLI} = 3.107\ km/s$
2. Lunar Orbit Insertion into a 100 km circular lunar orbit: $\Delta V_{LOI} = 0.819\ km/s$

Additionally, a ΔV reserve must be included to account for mid-course correction maneuvers (TCM), trajectory dispersions, and uncertainties during the translunar coast phase. Historical lunar missions allocated tens to hundred of meters per second for these maneuvers [3]. For this preliminary vehicle design, a conservative 150 m/s margin is allocated.

Mission ΔV Budget		
Segment	**ΔV (km/s)**	**Description**
Trans-Lunar Injection (TLI)	3.107	transfer injection
Lunar Orbit Insertion (LOI)	0.819	Capture into lunar orbit
Mid-course correction maneuvers (TCMs)	0.070	Small trajectory corrections
Injection/navigation/operation Reserve	0.080	Design contingency
Total	**4.076**	

Table 1. Mission Δv budget for transfer from 400 km LEO to a 100 km LLO.

The total required Δv for the mission was calculated to be 4.076 km/s, which includes all maneuver requirements and conservative loss estimates. This value is consistent with typical direct translunar transfers from LEO to low lunar orbit, which generally require approximately 4–5 km/s depending on trajectory design and correction requirements [2].

1.3 Staging Trade Study

With the mission Δv requirement established, a staging trade study was conducted to determine the most mass-efficient vehicle architecture. Structural coefficients were assumed based on typical values reported in literature for liquid rocket stages ($\epsilon = 0.08 - 0.15$) [4,5]. Staging enables the vehicle to discard inert structural mass after major propulsion events, improving overall mass efficiency. An initial staging trade

study was conducted using estimated propulsion parameters. An initial trade study was conducted using estimated propulsion parameters and later refined using final propulsion data from Roles 2 and 3.

Option A: Single-Stage Restartable Vehicle

Option A includes a single stage that performs all mission maneuvers. This configuration simplifies the system integration and eliminates staging, reducing mechanical complexity and potential failure points. However, this also means that the stage must carry the full propellant load and structural mass throughout the entire mission, including the translunar coast phase. This significantly increases the required initial mass in LEO.

Option B: Two-Stage Vehicle (Selected Design)

Option B is a two-stage system that separates the translunar injection and lunar orbit insertion maneuvers. Stage 1 performs the TLI burn and is discarded immediately afterward. Stage 2 is a restartable upper stage that performs LOI and provides Δv margin. By discarding Stage 1, the vehicle avoids carrying unnecessary structural mass to the Moon, which significantly improves mass efficiency.

Staging Trade Study Results					
Configuration	**Initial Mass in LEO (kg)**	**Initial Mass Reduction (%)**	**Total Propellant Mass (kg)**	**Total Structural Mass (kg)**	**Complexity**
Single Stage (A)	306.93	-	228.67	28.26	Low
Two Stage (B)	229.75	25.15%	161.55	18.2	Medium

Table 2. Quantitative staging trade study comparing single-stage and two-stage lunar transfer architectures.

The two-stage configuration reduces the required initial mass by 77.18 kg (25.15%), which represents a substantial improvement in mission efficiency. Although it introduces additional staging complexity, the mass savings and improved Δv efficiency make it the preferred architecture. Based on the results of this trade study, the two-stage architecture was chosen as the selected configuration for the remainder of the design process.

1.4 Final Stage ΔV Allocation

For the selected two-stage architecture, the total mission Δv of approximately 4.076 km/s was split between stages, reflecting the sequence of events rather than. The Δv contribution from each stage was determined using the rocket equation $\Delta V_i = I_{sp,i} g_0 ln(\frac{m_{0,i}}{m_{f,i}})$.

- **Stage 1 (TLI stage)** provides the majority of the Δv required to escape Earth orbit and inject the spacecraft onto a translunar trajectory.
- **Stage 2 (LOI stage)** provides the remaining Δv required for lunar orbit insertion and includes additional margin for trajectory corrections and uncertainties.

Final Stage ΔV Allocation			
Stage	**Function**	**ΔV (km/s)**	**Isp (s)**

Stage 1	Trans-Lunar Injection (TLI)	3.107	331.52
Stage 2	LOI + Reserve (Restartable)	0.969	304.15
Total	**-**	**4.076**	

Table 3. Final stage Δv allocation and propulsion performance for the selected two-stage architecture.

This ensures that the translunar injection maneuver is performed by the lower stage, minimizing the mass carried forward into later mission phases and improving overall vehicle efficiency.

1.5 Mass Breakdown and Refined Vehicle Design

Following the selection of the two-stage architecture, the vehicle design was updated using propulsion performance parameters provided by the propulsion and thermochemistry analyses. Stage mass ratios were recomputed using the refined propulsion parameters to ensure consistency with the Δv allocation. Structural coefficients were selected based on values for similar liquid rocket stages [4], [5]. Based on these ranges, values of $\varepsilon_1 = 0.10$ for the LOX/RP-1 first stage and $\varepsilon_2 = 0.11$ for the restartable NTO/MMH upper stage were selected. Stage mass properties were then determined using the rocket equation and different mass definitions.

$$\Delta V_i = I_{sp,i} g_0 ln(MR_i)$$

$$MR_i = \frac{m_{0,i}}{m_{f,i}}$$

$$\epsilon_i = \frac{m_{s,i}}{m_{s,i}+m_{p,i}}$$

$$m_{0,i} = m_{p,i} + m_{s,i} + m_{0,i+1}$$

$$m_{f,i} = m_{s,i} + m_{0,i+1}$$

Updated Propulsion Inputs				
Stage	**Propellant**	**Isp (s)**	**Structural Coefficient**	**ΔV (km/s)**
Stage 1	LOX/RP-1	331.52	0.1	3.107
Stage 2	NTO/MMH	304.15	0.11	0.969

Table 4. Updated propulsion inputs and structural coefficients used in the refined two-stage mass sizing analysis.

Refined/Finalized Mass Budget	
Component	**Mass (kg)**
Payload	50.00
Stage 2 Propellant	20.15
Stage 2 Structure	2.49
Stage 1 Propellant	141.40
Stage 1 Structure	15.71
Total Propellant Mass	161.55
Total Structural Mass	18.20
Total Initial Mass (LEO)	229.75

Table 5. Final vehicle mass budget for the selected two-stage architecture.

The refined two-stage architecture results in a total initial mass of 229.75 kg, which represents an improvement over our preliminary estimate. The majority of the propellant mass is allocated to Stage 1, reflecting its role in providing the higher Δv TLI requirement. Stage 2 performs a lower Δv maneuver and benefits from a higher specific impulse propellant combination (NTO/MMH) and a restartable engine design. This allows for both accurate orbital insertion and trajectory correction. The mass distribution demonstrates strong consistency with the Δv allocation and propulsion performance. The inclusion of a Δv margin further ensures robustness against modeling uncertainties and trajectory dispersions.

1.6 Trajectory Analysis Methodology

The trajectory analysis was performed using an orbital mechanics based approach. The objective was to determine whether our designed vehicle architecture could deliver a 50 kg payload from a 400 km circular Low Earth Orbit (LEO) to a 100 km circular Lunar Low Orbit (LLO), while also quantifying the remaining maneuver capability of the final stage. A Stage-1 full-burn was used, in which the entire Δv capability of Stage 1 is applied as an impulse burn. The resulting Earth-centered transfer is then determined using orbital mechanics, and the required Δv for lunar orbit insertion (LOI) is computed based on the arrival conditions at the Moon [6]. This approach ensures that the trajectory is directly consistent with the propulsion system performance.

To simplify the analysis, the following assumptions were made:

1. The trajectory is modeled as a two-body system
2. No Δv is explicitly used on midcourse corrections and operational margins
3. The spacecraft is assumed to achieve ideal targeting at arrival

Any remaining Δv after lunar orbit insertion is therefore interpreted as available operational margin for trajectory corrections and mission operations.

1.7 Stage ΔV Capability

The propulsive capability of each stage was calculated using the rocket equation. Stage 1 is responsible for the TLI and has a Δv capability of 3.107 km/s, while Stage 2 is responsible for LOI + margin, and has a capability of 0.969 km/s.

1.8 Stage-1 Full-Burn Translunar Transfer

The spacecraft begins in a 400 km circular Low Earth Orbit. The orbital velocity at this altitude is determined using the standard circular orbit relation: $v_{LEO} = \sqrt{\frac{\mu_E}{R_{LEO}}}$. This yields an initial orbital velocity of $v_{LEO} = 7.669\ km/s$. The first stage then applies its full ΔV capability $\Delta v_1 = 3.107\ km/s$. Resulting in a post-burn velocity of: $v_{burn,1} = v_{LEO} + \Delta v_1 = 10.776\ km/s$.

The resulting Earth-centered transfer trajectory is determined using the vis-viva equation, $v^2 = \mu_E(\frac{2}{r} - \frac{1}{a})$ [6] . This also gives semi-major axis of the transfer orbit gives, $a = 265,446\ km$. This corresponds to an apogee radius of $r_{apogee} = 524,115\ km$. Since this exceeds the Moon's orbital radius ($\sim 384,400\ km$), the spacecraft will intercept the Moon prior to apogee.

At the Moon's orbital radius the spacecraft velocity is $v_{transfer} = 0.756\ km/s$. The Moon's orbital velocity around Earth is $v_{moon} = 1.018\ km/s$. The hyperbolic excess velocity is therefore $v_\infty = |v_{transfer} - v_{moon}| = 0.262\ km/s$. This relatively low arrival velocity indicates that the Stage-1 full-burn trajectory produces a transfer that is slightly more energetic than a classical Hohmann transfer, but still results in a manageable lunar approach speed [6].

1.9 Lunar Orbit Insertion

After entering the Moon's sphere of influence the spacecraft follows a hyperbolic approach trajectory. The velocity at perilune is determined using $v_p = \sqrt{v_\infty^{\ 2} + \frac{2\mu_M}{r_p}}$, where μ_M is the lunar gravitational parameter, and r_p is the perilune radius [6]. With a target altitude of 100 km the perilune velocity is $v_p = 2.325\ km/s$. The circular velocity at this altitude is $v_{circ} = \sqrt{\frac{\mu_M}{r_p}} = 1.634\ km/s$. The required lunar orbit insertion burn is therefore $\Delta v_{LOI} = v_p - v_{circ} = 0.691\ km/s$.

1.10 Stage 2 Performance and Remaining Capability

The second stage provides a total Δv capability of $\Delta v_2 = 0.969\ km/s$. This exceeds the required LOI Δv of 0.691 km/s, leaving a remaining $\Delta v_{remaining} = 0.278\ km/s$. After completing the LOI burn, the propellant used was $m_{p2,used} = 15.03\ kg$. The burn duration was approximately $t_{burn} \approx 186\ s$. The remaining Δv of 0.278 km/s represents approximately 5.12 kg of propellant and 63 seconds of burn time

remaining. This excess capability can be used for trajectory correction maneuvers, orbital adjustments and extended mission operations

1.11 Trajectory Validation and Summary

Using this method the translunar transfer was derived directly from the available propulsion capability. This ensures full consistency between the system design and the resulting trajectory. The resulting trajectory reaches the Moon with a hyperbolic excess velocity of 0.262 km/s, requiring 0.691 km/s for lunar orbit insertion into a 100 km circular orbit. Since the second stage provides 0.969 km/s, the vehicle retains 0.278 km/s of additional capability. This confirms the selected architecture can deliver the payload to lunar orbit while maintaining Δv margin for maneuvers and mission operations.

---

2. Propulsion System Designer (Role 2)

---

2. Propulsion System Design Overview

The propulsion system design was performed using thermochemical properties obtained from the NASA Chemical Equilibrium with Applications (CEA) analysis performed in Role 3. These values include the chamber temperature, specific heat ratio, and molecular weight. We also found an iterated maximum vacuum specific impulse for each propellant combination. These properties were used with ideal isentropic rocket nozzle relations to determine thrust performance, nozzle geometry, and combustion chamber sizing.

Both propulsion stages operate primarily in vacuum conditions. Therefore, nozzle expansion ratios were selected to maximize vacuum performance. The propulsion system was designed at a preliminary level using characteristic velocity, thrust coefficient, expansion ratio, and combustion chamber characteristic length.

Since both propulsion stages operate in vacuum for the entirety of the mission, expansion ratios were optimized for vacuum performance rather than sea-level operation.

2.1 Stage 1 Engine

Stage 1 uses a **LOX/RP-1 bipropellant liquid rocket engine**. This propellant combination was selected because it provides relatively high thrust and good performance while maintaining a compact propellant volume due to the high density of RP-1. These characteristics make it well suited for the large burn required for the Trans-Lunar Injection (TLI) maneuver.

A **pump-fed liquid rocket engine** configuration was selected for Stage 1. Pump-fed engines allow significantly higher chamber pressures than pressure-fed systems, resulting in improved thrust and specific impulse. Higher chamber pressure increases the mass flow rate through the nozzle throat, which directly increases thrust according to the rocket thrust equation

$$T = \dot{m}V_e + A_e(p_e - p_a)$$

2.2 Stage 2 Engine

Stage 2 uses a **NTO/MMH hypergolic bipropellant engine**. This propellant combination is commonly used in spacecraft propulsion because it is storable at room temperature and ignites spontaneously when the oxidizer and fuel contact each other. These characteristics make hypergolic propellants highly reliable for in-space maneuvering and restartable engines.

Stage 2 was designed as a **pressure-fed rocket engine**. Pressure-fed systems are mechanically simpler than pump-fed systems because they do not require turbomachinery. This simplicity increases reliability, which is particularly valuable for spacecraft engines that must perform multiple restarts during critical mission maneuvers such as Lunar Orbit Insertion (LOI).

2.3 Mass Flow Rate and Thrust Determination

The burn time for each stage was calculated to be 283 s and 250 s respectively. The propellant masses were determined from the vehicle mass budget. Using these values, the propellant mass flow rate was determined from the mass conservation relation

$$\dot{m} = \frac{m_b}{t_b}$$

The thrust produced by each stage was then calculated using the relation

$$T = I_{sp} g_0 \dot{m}$$

Stage 1 thrust:

T = (332)(9.81)(0.499) = 1625.20 N

Stage 2 thrust:

T = (304)(9.81)(0.0807) = 240.67 N

2.4 Nozzle Expansion Ratio and Exit Conditions

The nozzle expansion ratio was determined by matching the calculated specific impulse from the isentropic nozzle equations with the vacuum specific impulse obtained from the CEA analysis. This ensures that the nozzle performance is consistent with the thermochemical properties of the propellant mixture.

The thrust coefficient in a vacuum is defined as:

$$C_{F,\text{vac}} = \sqrt{\frac{2\gamma^2}{\gamma-1}\left(\frac{2}{\gamma+1}\right)^{\frac{\gamma+1}{\gamma-1}}\left[1-\left(\frac{p_e}{p_0}\right)^{\frac{\gamma-1}{\gamma}}\right]} + \frac{A_e}{A_t}\frac{p_e}{p_0}$$

Using the CEA thermodynamic parameters and solving for the expansion ratio that produces the required specific impulse resulted in

Expansion ratio:

Stage 1: A_e/A_t = 65 Stage 2: A_e/A_t = 38

2.5 Nozzle Throat Area

The nozzle throat area was determined using the definition of characteristic velocity

$$c^* = \frac{P_0 A_t}{\dot{m}}$$

Using the chamber pressure P_c = 20 bar for stage 1, P_c = 12 bar for stage 2, and the CEA characteristic velocity values produced

Throat area:

Stage 1: A = 426 mm^2 Stage 2: A = 108 mm^2

2.6 Combustion Chamber Sizing

The combustion chamber was sized using the characteristic length relation

$$L^* = \frac{A_c}{A_t} L_c = \frac{V_c}{A_t}$$

where V_c is the chamber volume.

Typical characteristic lengths depend on propellant chemistry. Hydrocarbon engines typically require larger characteristic lengths than hypergolic engines due to slower reaction kinetics.

The following values were selected:

Stage 1 (LOX/RP-1):

L*=1.0 m

Stage 2 (MMH/NTO):

L*=0.6 m

The chamber contraction ratio was chosen as

$$CR = \frac{A_c}{A_t} = 4$$

Using this contraction ratio, the combustion chamber length becomes

$$L_C = \frac{L^*}{CR}$$

resulting in chamber lengths of

Stage 1: L_c = 0.25 m Stage 2: L_c = 0.15 m

2.7 Nozzle Contour Selection

Two nozzle contour options were considered for both stages: a conical nozzle and a bell nozzle. A conical nozzle is simpler to design and manufacture, but it suffers from divergence losses because a portion of the exhaust leaves the nozzle at an angle rather than purely in the axial direction. The thrust correction factor for the momentum term in conical nozzles is

$$\lambda = \frac{1 + \cos(\alpha)}{2}$$

where alpha is the conical half-angle. For a typical 15 degree conical nozzle, this gives 0.98296

The momentum thrust loss is about 1.7% relative to perfectly axial flow. Conical nozzles are also relatively long for a given area ratio. NASA's liquid rocket nozzle design monograph shows that simple straight-wall conical nozzles are easy to manufacture and are commonly found on smaller rockets, while bell nozzles are used on larger flight systems. It also defines an "80% bell" as a bell nozzle whose length is 80% of the length of an equivalent 15° half-angle conical nozzle with the same area ratio [12].

A bell nozzle reduces divergence losses by turning the exhaust more gradually so the exit flow is axial, while also shortening the nozzle compared with a conical design. NASA reports that bell nozzles are contoured for optimum performance within a certain length, and that performance isn't sensitive to small deviations from the optimum contour [11]. In addition, a NASA design report for an optimized vacuum nozzle found an optimum vacuum nozzle length of 75.2% of the equivalent conical length, while the final

design envelope used an 80% bell, which is very close to that optimum and reflects standard practice for high-area-ratio vacuum nozzles [12].

Based on this trade, **an 80% bell nozzle was selected for both propulsion stages**. This choice provides a good compromise between performance and mass: it avoids the extra length and divergence loss associated with a conical nozzle, while remaining simpler to specify at the preliminary design level, rather than a fully optimized contour. Since both of our stages operate primarily in vacuum, the bell nozzle is the more appropriate choice [11], [12].

2.8 Performance Summary Table

Parameter	Units	Stage 1	Stage 2
Thrust	N	1620.20	241.67
Chamber Pressure	bar	20	12
Burn Time	s	283	250
Mass Flow Rate	kg/s	0.499	0.0807
Characteristic Velocity c*	m/s	1710	1600
Thrust Coefficient CF	-	1.9	1.86
Specific Impulse Isp	s	332	304
Exit Area Ratio Ae/At	-	65	38
Exit Mach Number Me	-	4.68	4.34
Exit Pressure Pe	bar	0.0212	0.0241
Exit Pressure Ratio Pe/Pc	-	0.00106	0.00201
Throat Area At	mm^2	426	108
Exit Area Ae	mm^2	27700	4180
Characteristic Length L*	m	1	0.6
Chamber Length Lc	m	0.25	0.15
Chamber Area Ac	mm^2	1700	431
Chamber Volume Vc	m^3	0.000426	0.0000647
Chamber Diameter Dc	m	0.0466	0.0234

Table 6. Engine performance and thermodynamic properties for Stage 1 and Stage 2.

---

3. Propellant and Thermochemistry Specialist (Role 3)

3.1 Stage 1 TLI Candidates:

Option 1: LOX / LH_2 (Hydrolox)

Research on Hydrogen as fuel started in the 1940s, but really took off in the late 1950s to early 1960s with the help of advances in cryogenic storage technology. Hydrolox has the highest specific impulse(Isp) of any practical chemical rocket, with an Isp around 450s. Hydrolox has a strong heritage and became the staple upper-stage propellant choice for hundreds of rockets. The prop is also being used for modern heavy-lift boosters that need high efficiency and can afford the technical hassle. The pitfall of this propellant is the need for cryogenic storage and its very low density causing the need for massive tanks. Historical examples include the upper stages of the Saturn V [4],[7],[9].

Option 2: LOX / LCH_4 (Methalox)

Methalox emerged as an attractive alternative to hydrolox and kerolox as engineers looked for a propellant combination that balanced performance, cleanliness, and operability. Although it is not as clean as hydrolox, it still burns cleaner than RP-1, producing less soot making it a better choice for reusable engines. Its main drawbacks are lower heritage than hydrolox or kerolox and lower density than RP-1.

Option 3: LOX/RP-1 (Kerolox)

Developed in the mid 1950s kerolox has the strongest heritage among all propellants with hundreds of historical uses like the Saturn V first stage for the Apollo missions. RP-1 is stable at surface ambient conditions making up for its lower efficiency by its ease of storage. RP-1 is roughly twice as dense as liquid methane making it an ideal choice when trying to maximize thrust to weight ratio or compactness by keeping tank size to a minimum [4].

3.2 Stage 2 LOI/ Restartable Stage:

Option 1 : NTO / MMH

NTO/MMH is a storable hypergolic propellant with a strong heritage that has been used for upper stages and deep-space maneuvers since the 1960s. Its biggest advantage is that it is hypergolic, meaning that the Nitrogen Tetroxide (NTO) and Monomethylhydrazine (MMH) ignite on contact. This allows simple restarts without a complex ignition system. It is also easier to store than cryogenic propellants, making it a better choice for long coast phases and orbital maneuvering stages. The primary downsides associated with the prop are its toxicity, which poses handling hazards. Historical examples include spacecraft propulsion systems and restartable orbital maneuver stages [4],[8].

Option 2: LOX / CH_4

Detailed propellant description given in the first-stage section.

Option 3: LOX / LH_2

Detailed propellant description given in the first-stage section.

3.3 CEA First Pass

An initial CEA case was run to get the characteristics (T0, γ, M) of each candidate propellant. The Oxidizer-to-Fuel (O/F) ratio was swept from 1-7 to find the ratio that gives you the peak Isp. The setting for the initial CEA are as follows:

- $P_c = 30_{\text{ba}}$
- $p_a \approx 0$
- $\epsilon = 100$

First Pass Results

LOX/LH2: peak at O/F = 4.75, Isp = 455.8 s, **Ivac = 468 s**

LOX/CH4: peak at O/F = 3.25, Isp = 367.3 s, **Ivac = 381 s**

LOX/RP-1: peak at O/F = 2.75, Isp = 356.3 s, **Ivac= 371 s**

NTO/MMH: peak at O/F = 2.25, Isp = 341.1 s , **Ivac = 353 s**

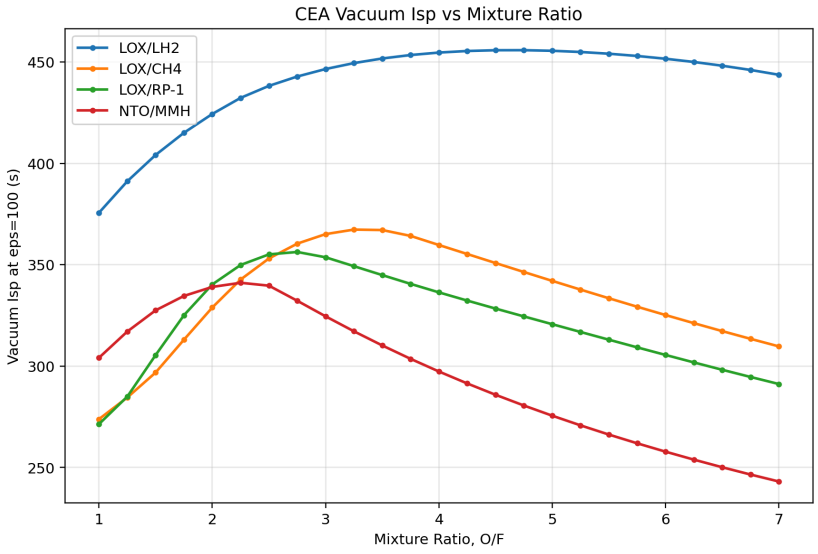

Figure 2. Vacuum specific impulse vs. Mixture Ratio for Propellent Candidates at $\epsilon = 100$

Propellant Selection and Trade Study Result

Using the CEA analysis and the qualitative table 7 seen below the team was able to select the propellant that balances performance, mission requirements, and engineering complexity.

Keralox was chosen as the propellant for stage 1. The biggest contributing factor to its selection over the other candidates is its much higher density. RP-1 is 11 times more dense than LH2 and about twice as

dense as LCH4. RP-1s high density aids in optimizing tank size to meet mission requirements of keeping the vehicle small. Even when factoring in bulk density using the O/F from the CEA for each prop, the difference in density between Methalox(814 kg/m^3) and Keralox(1026 kg/m^3) becomes much closer but for Methalox you would still need a tank about 25% larger. The slighter higher Isp of Methalox is not enough to overcome the tank size discrepancy. The main detractor of Keralox when compared to the other two candidates is the toxicity, but since the burns are occurring in LEO and beyond its acute toxicity during burns was not a factor in the selection. While there are handling hazards, keralox benefits from a longer operational history, which has reduced technical and operational risks. Finally RP-1 has the strongest heritage of all propellants, it is a proven cost efficient propellant with decades of engineering work and research behind it.

MMH/NTO was selected as the propellant for stage 2 because it best aligns with the mission's wants and requirements. To begin with, MMH/NTO excels in the storability department. Since the second stage must coast after TLI and then reliably perform LOI, the propellant combination needed to remain usable without the boiloff and thermal management challenges associated with cryogenic systems. Since MMH/NTO is storable at near-ambient conditions it is the best suited selection for this coast phase. The next major factor is MMH/NTO’s hypergolic property, using this prop combination gives the team a strong advantage for designing a restartable upper-stage without a complex ignition system. Lastly, MMH/NTO is much denser than Hydrolox and Methanlox aiding in keeping our 2nd stage compact. Overall the “simpler” nature of Hydrazine systems are easier operationally and are often more cost effective. Like Keralox but to an even greater extent, MMH/NTOs greatest disadvantage is its toxicity. For this mission this mainly would involve the handling hazards since the burns will be performed in space. For this mission the benefits in storability, restart reliability and simplicity, and compact tankage outweighed that drawback.

Stage	Candidate	Heritage	Vacuum performance	Storability	Restart ease	Toxicity	Relative tank size	Overall fit
1/2	LOX/LH2	High	Excellent	Poor	Moderate	Low	Large	Good
1/2	LOX/CH4	Moderate	Very good	Good	Moderate	Low	Medium	Good
1	LOX/RP-1	Very high	Good	Fair	Moderate	Moderate	Small	Very good
2	NTO/MMH	Very high	Good	Excellent	Excellent	High	Small	Excellent

Table 7. Qualitative Properties of Propellent Candidates

3.4 Second CEA Sweep: Chamber Pressure and Area Ratio Analysis

2nd Sweep Case:

Stage 1 LOX/RP-1

- $P_c = 20,30,40\text{bar}$

Stage 2 NTO/MMH

- $P_c = 8,12,15\text{bar}$

Case Rational:

The pressure and area ratios for the cases were selected based on historical design points from NASA. For the 1st stage chamber pressure we used NASA's RL10A-3-3 as a reference which used 27.6 Bar. For the 2nd stage we used the chamber pressure from the Apollo Service Propulsion System engine of 6.9 Bar as a reference along with a general pressure fed range [7],[8].

3.5 Final CEA Results:

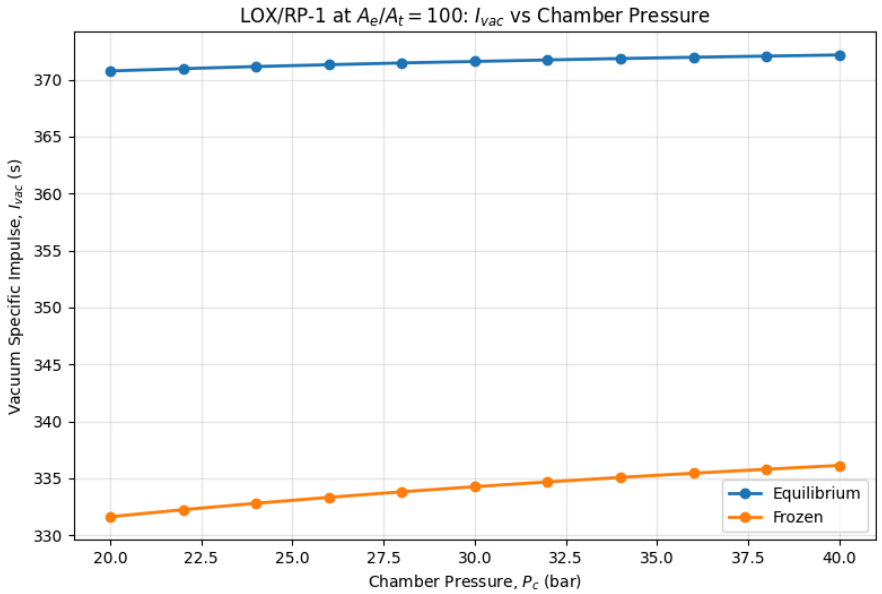

Figure 3. Vacuum specific impulse vs. chamber pressure for LOX/RP-1 at ϵ=55

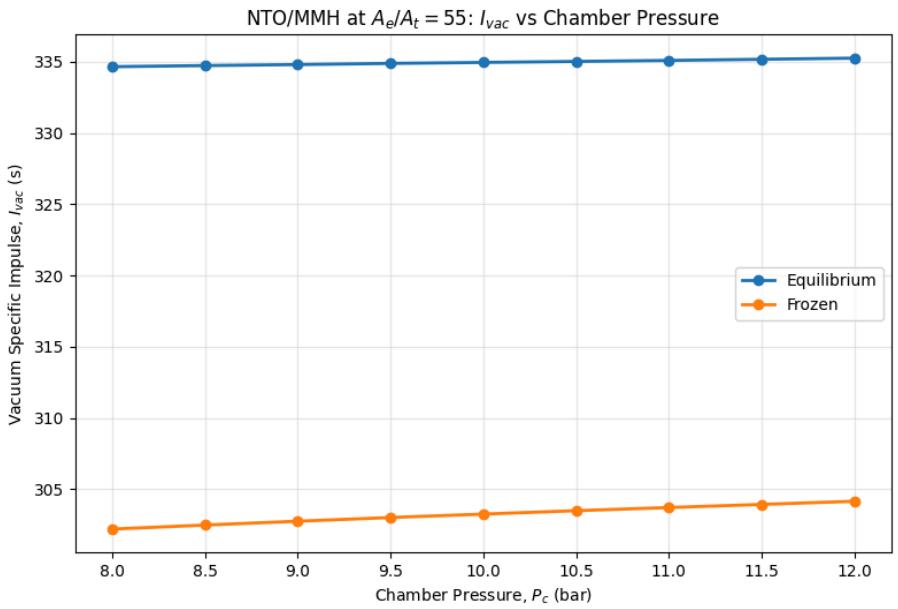

Figure 4. Vacuum specific impulse vs. chamber pressure for NTO/MMH at ϵ=55

RP-1/LOX Final values at selected Chamber pressure of 20 Bar. We selected the bottom end of the pressure range because the increase in Isp was marginal when you increase the pressure.

Frozen

- $T_0 = 3506.20$ K
- $M = 23.576$
- $\gamma = 1.2145$
- $I_{sp} = 3142.8$ m/s $= 320.48$ s
- $I_{vac} = 3252.2$ m/s $= 331.63$ s

MMH/NTO Final values at selected Chamber Pressure of 12 Bar. This pressure was selected because the lower end pressures while resulting in usable Isp values also resulted in too large “ideal” exit to throat area ratios.

Frozen

- $T_0 = 3167.90$ K
- $M = 24.047$
- $\gamma = 1.2207$
- $I_{sp} = 2888.2$ m/s $= 294.51$ s
- $I_{vac} = 2982.8$ m/s $= 304.15$ s

3.6 CEA Frozen Vs Equilibrium

Due to our nozzle type being bell and having a small characteristic length along with our vehicle being relatively small frozen CEA values are more realistic. This is due to the nozzle residence time being relatively low for these types of nozzle. With the low residence time the exhaust gases never reach equilibrium. Using the frozen values gives us a smaller magnitude in Isp and Ivac but facilitates a more realistic design [4].

---

4. Systems Integration & Broader Impacts Lead (Role 4)

The mission requires delivering a 50Kg payload from a Low Earth Orbit (LEO) parking orbit to a low lunar orbit of 100km. From the mission analysis, the propulsion system must deliver 4.076 km/s total ΔV. To meet this requirement, a two-stage system has been selected. Stage 1 will perform the Trans-Lunar Injection (TLI) burn, and stage 2 will perform the lunar orbit insertion maneuver. Separating the Trans-Lunar burn from the orbit insertion maneuver allows the inert structural mass of stage 1 to be jettisoned after TLI, improving overall efficiency.

Stage 1 uses a LOX/RP-1 pump-fed system that provides the needed high thrust for the TLI burn, as well as high performance. Stage 2 uses a pressure-fed NTO/MMH engine that provides reliable hypergolic ignition, restartable ignition, and long-term storability.

4.1 Mass Budget Closure

The mass budget for this vehicle configuration was calculated using the specific impulse values and structural fractions.

Component	**Mass (kg)**
Payload	50.00
Stage 2 propellant	20.15
Stage 2 structure	2.49
Stage 1 propellant	141.39
Stage 1 structure	15.71

Table 8. Mass budget for the proposed two-stage vehicle.

Total initial mass:

$$m_0 = 50 + 20.15 + 2.49 + 141.39 + 15.71 = 229.75\,kg$$

4.2 Thrust-to-Weight

Because this translunar vehicle is assumed to begin its mission in a low Earth parking orbit, it does not perform a launch from the ground; therefore, the thrust-to-weight ratio (T/W)≥ 1.2 applies only to the launch vehicle. Compared to the Apollo mission, a T/W of 0.72 was calculated for the TLI burn, and a T/W of 0.338 was calculated for the orbit insertion maneuver.

Apollo Values

Apollo TLI stack mass[13]:

$$m = 146,250\ kg$$

Weight:

$$W = mg = 146,250 * 9.80665 = 1,434,222.56\ N$$

Thrust[14]:

$$T = 1,033,000\ N$$

$$T/W = \frac{1,033,000}{1,434,000} = 0.72$$

Apollo orbit insertion stack mass:

$$m = 12,250 + 15,200 = 27,450\ kg$$

Weight:

$$W = 27,450 * 9.80665 = 269,192.54\ N$$

Thrust:

$$T = 91,000$$

$$T/W = \frac{91,000}{269,192.54} = 0.338$$

Proposed Vehicle

Stage 1 (TLI)

$$T = (T/W) * W = 0.72 * (229.75 * 9.80665)$$

$$T = 1622.21\ N$$

Stage 2 (LOI)

$$T = (T/W) * W = 0.338 * (72.64 * 9.80665)$$

$$T = 240.77\ N$$

4.3 Stage Interfaces

Stage 1 is connected to stage 2 via an interstage adapter that transfers the loads during the translunar injection burn. This adapter must support axial loads from the thrust and maintain alignment with the upper spacecraft structure. After the TLI burn is completed and all propellant is depleted, stage 1 is released so its structural mass is not carried to the Moon.

Stage 2 remains attached to the payload during the coasting phase of the TLI and the lunar orbit insertion maneuver. The 50 kg payload is mounted to stage 2 using a payload adapter that must support the loads experienced during launch and the trans-lunar burn. The payload adapter must accommodate the deployment of the payload upon arrival.

Vehicle Specification Table

Parameter	**Stage 1**	**Stage 2**	**Overall Vehicle**
Primary Function	Trans-Lunar Injection (TLI)	Lunar Orbit Insertion (LOI) + reserve	Deliver 50 kg payload to a 100 km LLO
Propellant	LOX/RP-1	NTO/MMH	Two-stage lunar transfer vehicle
Engine feed system	Pump-fed	Pressure-fed	–
Restartability	No	Yes	Restart required for the upper stage
ISP,vac (s)	331.52	304.15	–
Structural Fraction ϵ	0.10	0.11	–
Mixture O/F	2.75	2.25	–
ΔV (km/s)	3.107	0.969	4.076
Propellant mass (kg)	109.33	16.82	136.52
Structural mass (kg)	12.15	2.08	14.23
Initial stage mass (kg)	190.38	68.90	190.38
Final mass after burn (kg)	81.05	52.08	50 kg payload delivered w/ hardware
Payload carried above stage (kg)	68.90	50.00	50.00
Mission phase	LEO to Trans-Lunar Injection (TLI)	Lunar Orbit Insertion (LOI)	LEO to 100 km LLO

Table 9. Summary of vehicle specifications for Stage 1, Stage 2, and the overall vehicle.

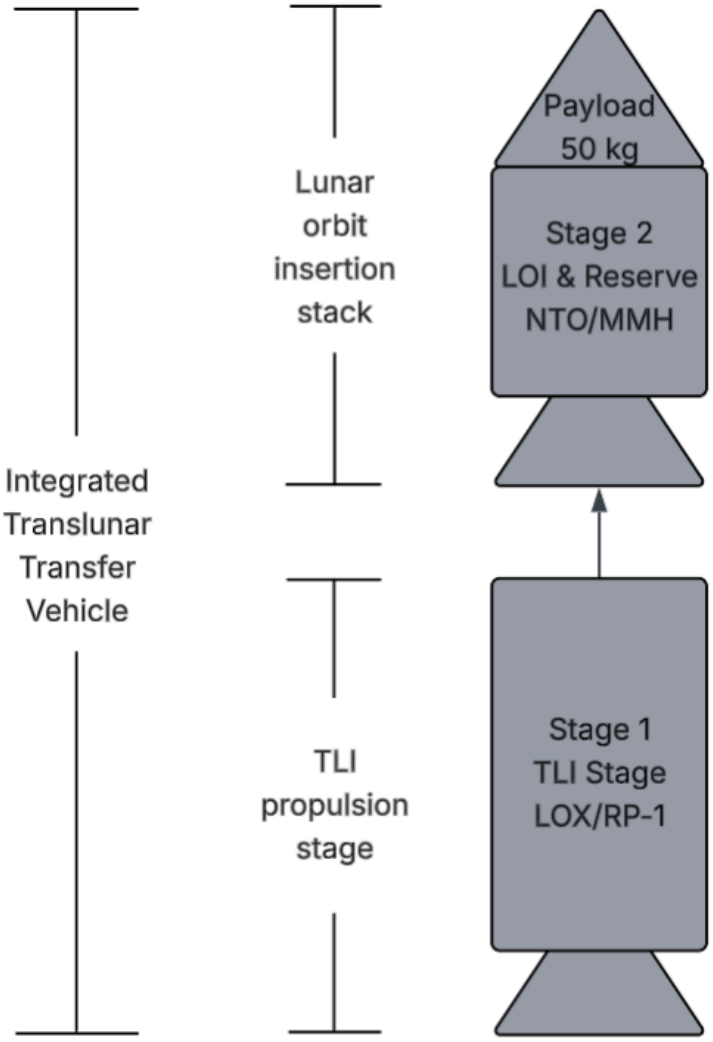

Figure 5. Two-stage translunar vehicle configuration

4.5 Environmental Impact

The trans-lunar injection burn performed by stage 1 uses a LOX/RP-1 propulsion system. The combustion of RP-1 produces carbon dioxide, water vapor, and soot particles. Because this burn begins in LEO, these byproducts are injected directly into Earth's upper atmosphere. Soot and carbon dioxide both influence atmospheric balance and chemistry [15]. Soot absorbs the incoming sunlight and heats the surrounding area, while carbon dioxide traps infrared radiation emitted from Earth's surface. However, at the high altitudes experienced during this burn, the extremely low atmospheric density limits the overall environmental impact from these products. Additionally, because this translunar vehicle begins in a low Earth parking orbit, it does not contribute to any launch noise or acoustic effects at the ground level.

The lunar orbit insertion maneuver performed by stage 2 uses an NTO/MMH propulsion system and occurs near the moon after the translunar coast phase. These exhaust byproducts do not specifically interact with Earth's atmosphere, but the propellant itself is highly toxic during fueling and other ground operations. Because nitrogen tetroxide (NTO) and monomethylhydrazine (MMH) are hypergolic, they require strict safety procedures during handling, fueling, or storage to avoid contact or releases.

After the TLI burn, stage 1 is discarded from the remaining vehicle structure while on the translunar trajectory. This means stage 1 will not re-enter Earth's atmosphere, but may impact the Moon (as seen with Saturn V), or enter a heliocentric orbit.

LOX/RP-1 exhaust composition (Stage 1)

Species	**Mass %**
CO2	49.891
H2O	27.773
CO	21.690
H2	0.641
OH	0.004

Table 10. Lox/RP-1 exhaust composition

NTO/MMH exhaust composition (Stage 2)

Species	Mass %
N2	39.78
H2O	31.82
CO2	25.32
CO	2.58
H2	0.48

Table 11. NTO/MMH exhaust composition

4.6 Societal and Global Context

Translunar vehicles capable of delivering small payloads support commercial, scientific, and national interests by providing access to lunar orbit. These missions can contribute to scientific understanding of the Moon, lunar mapping, and technology demonstrations. A smaller, low-cost payload delivery system allows private companies, research groups, or universities to participate in lunar missions that have been limited to large government programs.

Small translunar vehicles support programs such as NASA's Commercial Lunar Payload Services (CLPS) and other lunar expedition programs by enabling affordable payload delivery.

4.7 Comparison with Apollo

Because this translunar vehicle begins its operation in a low Earth parking orbit, comparing it to a traditional ground launch vehicle is not suitable. A more relevant comparison is the Apollo Program, which used similar mission phases. To ensure a realistic behavior of both stages in the translunar vehicle, the thrust levels were determined by matching the Apollo mission phase thrust-to-weight ratios. Using this design parameter, the proposed translunar vehicle achieves a similar behavior to Apollo despite operating at a much smaller scale.

The translunar injection phase of the translunar vehicle has an initial mass of 229.75 kg and produces a thrust of 1622.15 N, yielding a thrust-to-weight ratio of 0.72. This matches the Apollo thrust-to-weight ratio of 0.72, achieved with a stack mass of 146,250 kg and a thrust of 1,033,000 N. The lunar orbit insertion phase has an initial mass of 72.64 kg and produces 240.78 N of thrust, yielding a thrust-to-weight ratio of 0.338. This ratio also matches the thrust-to-weight ratio achieved by Apollo's lunar orbit insertion stage with a mass of 27,450 kg and a thrust of 91,000 N.

Using the thrust-to-weight ratios provides this translunar vehicle with burn times of 283.5 seconds for trans lunar injection and 249.7 seconds for low orbit insertion. Although these values aren't identical to

Apollos' burn times of 345 and 357.5 seconds, they are within the same operational range, supporting realistic engine sizing.

Environmentally, the comparison between these two vehicles differs drastically. Because the proposed vehicle launches from a low Earth orbit, it does not contribute to launch site noise or air quality effects and primarily contributes to emissions in the upper atmosphere. The first stage (LOX/RP-1) produces carbon dioxide, water vapor, carbon monoxide, and small amounts of soot as the main combustion products. The second stage uses a hypergolic mix of NTO/MMH, which are highly toxic at ground level, but because the combustion occurs entirely in space, the environmental impacts from the exhaust are negligible.

Proposed Vehicle

Mission phase	Stage 1 (TLI)	Stage 2 (LOI)
Initial mass (kg)	229.75	72.64
Propellant mass (kg)	141.39	20.15
Structure mass (kg)	15.71	2.49
Thrust (N)	1622.15	240.78
T/W	0.72	0.338
Burn time (s)	283.50	249.70

Apollo

Mission phase	TLI	LOI
Stack mass (kg)	146,250	27,450
Thrust (N)	1,033,000	91,000
T/W	0.72	0.338
Burn time (s)	345.00	357.5

Table 12. Performance comparison between the proposed vehicle and the Apollo mission phases.

Conclusion & Recomendations

Overall, the proposed two-stage translunar vehicle meets the requirements of delivering a 50kg payload from a low Earth parking orbit to a 100km low lunar orbit. This vehicle meets the required total ΔV of 4.076 km/s by using a multi-stage design that separates the translunar injection from the lunar orbit insertion maneuvers. The selected propulsion system works well for this mission. The LOX/RP-1 pump-fed first stage provides the required thrust for the TLI maneuver, and the pressure-fed NTO/MMH system provides reliable ignition and restart capabilities for the lunar orbit insertion maneuver.

The biggest risk with the design of this vehicle is the use of a pump-fed LOX/RP-1 system. This pump-fed system may increase the difficulty of development and reliability at such a small scale. Another risk is the use of a hypergolic system. While reliable and restartable, this system uses highly toxic propellants that require strict handling procedures during ground operations.

With more time, several areas of this mission design could be further improved. A more refined trajectory analysis would further improve the accuracy of the ΔV requirements and burn timing. Additional focus could be made on the structural design, including the modeling of the tanks and feed systems. Finally, a complete system integration of guidance, navigation, and control would be necessary to ensure overall mission reliability.

References

[1] B. He, S. Wu, and H. Li, "Reachable set analysis of practical trans-lunar orbit via a retrograde semi-analytic model," Earth, Planets and Space, vol. 75, no. 34, 2023.

[2] NASA COMPASS Team, Lunar Lander Concept Study, NASA Technical Reports Server, 2011.

[3] A. B. Binder, "Lunar Prospector mission and spacecraft design," NASA Ames Research Center, 1998.

[4] G. P. Sutton and O. Biblarz, Rocket Propulsion Elements, 9th ed. Hoboken, NJ: Wiley, 2017.

[5] D. K. Huzel and D. H. Huang, Modern Engineering for Design of Liquid-Propellant Rocket Engines, NASA SP-125, National Aeronautics and Space Administration.

[6] M. A. Sharaf, A. N. Saad, and M. I. Nouh, "Transfers to low lunar orbits," JPL DESCANSO Monograph Series.

[7] Pratt & Whitney Aircraft, RL10 Design Report, RL10A-3-3, 1966.

[8] C. R. Gibson, Service Propulsion Subsystem, NASA, 1973.

[9] NASA, Launch Vehicles / Saturn launch vehicle history.

[10] M. Binder, RL10A-3-3A Rocket Engine Modeling Project, NASA, 1997

[11] Rao, G. V. R., "Exhaust Nozzle Contour for Optimum Thrust,"

NASA Technical Note D-293, National Aeronautics and Space Administration, 1958.

[12] Sutton, G. P., and Biblarz, O., Liquid Rocket Engine Nozzles,

NASA SP-8120, National Aeronautics and Space Administration, 1976.

[13] NASA, Apollo by the Numbers: A statistical Reference, NASA SP-4029

[14] NASA, Apollo 11 Press Kit, National Aeronautics and Space Administration, 1969.

[15] S. P. Sharma, Impact of Spaceflight on Earth's Atmosphere: Climate, Ozone, and the Upper Atmosphere, NASA, 2024